

# Charged particle reflection in a magnetic mirror

L. A. Fernández-Ramos<sup>a</sup>, J. E. Mendoza-Torres<sup>b</sup>, O. Gómez-Flores<sup>a</sup> and E. Tirado-Bueno<sup>a</sup>

<sup>a</sup>Space Science and Technology Department, Instituto Nacional de Astrofísica, Óptica y Electrónica, Calle Luis Enrique Erro No.1, Santa María Tonantzintla, Puebla, 72840, Puebla, e-mails: lfernandez@inaoep.mx; octavio.gomez@inaoep.mx; etirado@inaoep.mx

<sup>b</sup>Astrophysics Department, Instituto Nacional de Astrofísica, Óptica y Electrónica, Calle Luis Enrique Erro No.1, Santa María Tonantzintla, Puebla, 72840, Puebla, e-mail: mend@inaoep.mx

Received 22 October 2023; accepted 8 January 2024

We study the reflection of electrons in a magnetic field mirror. It is a field with a gradient from the lowest value  $B_0$  to the largest one  $B_m$ . With this purpose, Montecarlo simulations are made. We use a number of 5,000 particles with random pitch angles. The frequency distribution of these random values follows a Gaussian distribution centered at  $\theta = 0$  and with standard deviation  $\sigma$ . Various values of  $\sigma$  and also different values of the  $B_0/B_m$  ratio are used in the simulations. The simulations show that  $\sigma$  has an important influence on the confinement of charged particles, for the different  $B_0/B_m$  ratios here studied. However, the percent of reflected particles differs from a  $B_0/B_m$  ratio to another in the whole range of  $\sigma$ , although for  $\sigma = 10$  the differences between different ratios are small ( $< 5\%$ ). The number of reflected particles increases very rapidly with  $\sigma$ , in the range of  $10^\circ$  to  $40^\circ$ . For the  $\sigma$  range from  $20^\circ$  to  $40^\circ$ , the percent of reflected particles is  $\geq 20\%$  larger for  $B_0/B_m = 0.10$  than for the 0.55 ratio.

**Keywords:** Magnetic mirror; Montecarlo; plasma.

DOI: <https://doi.org/10.31349/RevMexFisE.21.020211>

## 1. Introduction

Natural scenarios where particles are trapped by magnetic fields  $B$  are seen in several objects, the atmospheres of planets, including the Earth, the Sun, pulsars, and in several Astronomical objects [1], where the interaction of charged particles with  $B$  is important. In the atmospheres of planets and at the Sun, magnetic loops are seen to be good scenarios to retain charged particles. In the Earth, the Van Allen Belts are one of such cases where high densities of charged particles are maintained at magnetic loops. However, in all these scenarios also a part of the particles precipitates and leaves the loops. The interaction of magnetic field and charged particles in the loops is important to understand why a part of the particles is retained while other left the loops. For instance, the performance of cyclotrons and other particle accelerators depends on the trapping of particles by magnetic fields while in some other cases, the confinement and further release of particles is of importance as in thrusters in space technology and also in the industry [2], as in the cases of welding machines and plasma cutting instruments.

The path of a charged particle in a homogeneous magnetic field  $B$  is the well-known helix, with its axis aligned to the  $B$  lines and where the particle traces circles in the perpendicular direction to the helix axis. Here we deal with the case of a magnetic field  $B$  whose strength is a function of  $z$ , with growing  $B$  as  $z$  grows. As below seen, we assume an ideal case of an ensemble of electrons that is released at the point with the lowest  $B$  and travels towards the direction of higher  $B$ .

## 2. A charged particle in a magnetic mirror

We consider ideal conditions of a magnetic field in free space, which has a gradient in the axial coordinate, with the lowest value  $B_0$  and the highest one equal to  $B_m$ . To represent this situation, a cylindrical geometry can be used. The region with a large magnetic field can act as a mirror for charged particles. In our case,  $B_0$  is in the middle and the magnetic field increases towards both sides. This scenario is referred to as a magnetic bottle [1]. In Fig. 1 a part of such a bottle is shown. We assume that a charged particle departs from the region with  $B_0$  and goes towards the region of  $B_m$ . The total force experienced by a moving charge is the Lorentz force, given by

$$\mathbf{F} = q(\mathbf{E} + \mathbf{v} \times \mathbf{B}), \quad (1)$$

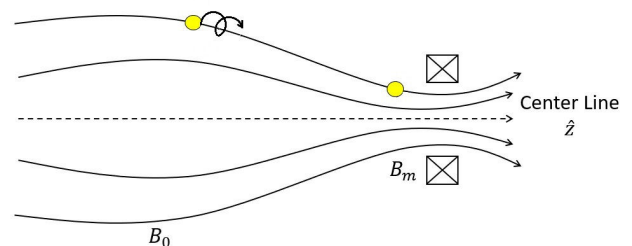


FIGURE 1. Representation of the magnetic field lines, in the case where the field has a gradient in the direction of the lines ( $\nabla B \parallel B$ ), where  $B_0$  and  $B_m$  represent, respectively, the minimum and maximum magnetic fields.

where  $q$  is the charge of the particle,  $\mathbf{v}$  is its velocity,  $\mathbf{E}$  and  $\mathbf{B}$  are the electric and magnetic fields, respectively. If we assume that there is no applied electric field, we only include the contribution of the magnetic field. In cylindrical coordinates, and taking into account that the component in theta is zero because we assume an axisymmetric geometry, the Eq. (1) results

$$\mathbf{F} = \hat{r}(qv_\theta B_z) + \hat{z}(qv_\theta B_r). \quad (2)$$

From Maxwell's equations, we know that the divergence of the magnetic field is zero. In cylindrical coordinates, the expression for the divergence of  $B$  is

$$\nabla \cdot B = \frac{1}{r} \frac{\partial r \partial B_r}{\partial z} + \frac{\partial B_z}{\partial z} = 0, \quad (3)$$

then

$$\frac{\partial r B_r}{\partial r} = -r \frac{\partial B_z}{\partial z}, \quad (4)$$

and

$$dr B_r = -r \frac{\partial B_z}{\partial z} dr. \quad (5)$$

Further, we can see that integrating Eq. (5), the radial component of the magnetic field can be expressed as a function of the axial component  $B_z$ , *i.e.*, in the direction of the axis of the cylinder, with a variable radius.

$$r B_r = - \int_0^r r \frac{\partial B_z}{\partial z} dr = - \frac{r^2}{2} \frac{\partial B_z}{\partial z}, \quad (6)$$

which leads to

$$B_r = - \frac{r}{2} \frac{\partial B_z}{\partial z}. \quad (7)$$

Then, we can also calculate the force that the particle experiences in the axial direction [ $z$  component of Eq. (2)], using Eq. (7)

$$F_z = qv_\theta \frac{r}{2} \frac{\partial B_z}{\partial z}. \quad (8)$$

The radial component of the magnetic force, given by Eq. (2), is

$$F_r = qv_\theta B_z. \quad (9)$$

The radial component of the force Eq. (9) is equal to the centripetal force that undergoes the particle [3], leading to the Eq. (10), as follows

$$qv_\theta B_z = - \frac{mv_\theta^2}{r}. \quad (10)$$

In its movement inside the magnetic bottle, the charged particle describes a helical trajectory [4]. On this trajectory, the gyro-radius (or Larmor radius) for an initial velocity and a component of the magnetic field  $B_z$  is given by

$$r_L = - \frac{mv_\theta}{qB_z}. \quad (11)$$

Substituting  $r_L$  from Eq. (11) into Eq. (8), we obtain

$$F_z = \frac{mv_\theta^2}{2B_z} \frac{\partial B_z}{\partial z}. \quad (12)$$

In Eq. (12), the term  $mv_\theta^2/2B_z$  represents the kinetic energy of the particle due to its rotation around the  $B$  lines, divided by the axial magnetic field. This ratio is equal to the force in the axis of the magnetic bottle. The potential energy of the particle is

$$U = -\mu \cdot \mathbf{B}, \quad (13)$$

where  $\mu$  is the magnetic dipole moment. Equation (13) implies that the energy is the lowest when the magnetic moment is aligned with the magnetic field. Due to the conservation of momentum [5], we have that

$$\frac{d\mu}{dt} = 0. \quad (14)$$

On the other hand, the angle of the particle path, respect to the  $z$  axis (the magnetic bottle axis), also referred to as pitch angle, can be expressed as

$$\sin \theta = \frac{v_\perp}{v}. \quad (15)$$

The gyroradius of the particle is determined by the perpendicular component of the velocity to the axis of the bottle [3], then the magnetic moment is

$$\mu = \frac{1}{2} \frac{mv_\perp^2}{B}, \quad (16)$$

where the perpendicular component of the velocity can be obtained from Eq. (15)

$$v_\perp = v \sin \theta. \quad (17)$$

Substituting Eq. (17) into (16) we obtain

$$\mu = \frac{1}{2} \frac{mv_\perp^2}{B} = \frac{1}{2} \frac{mv^2 \sin^2 \theta}{B}. \quad (18)$$

We can divide Eq. (18) by the kinetic energy of the particle, which in this case is also conserved [3]. Therefore, the  $\sin^2 \theta/B$  ratio is the same at the location of the minimum magnetic field  $B_0$ , where the particle's pitch angle is  $\theta_0$ , and in any other location (where the magnetic field is  $B$  and the pitch angle is  $\theta$ ). Then, when the particle is at the magnetic field maximum  $B_m$ , the next equality is fulfilled.

$$\frac{\sin^2 \theta}{B_m} = \frac{\sin^2 \theta_0}{B_0}. \quad (19)$$

The critical condition for the particle to be reflected at the position of  $B_m$  is

$$\theta > 90^\circ. \quad (20)$$

On the other hand, if the angle at that position is

$$\theta < 90^\circ, \quad (21)$$

then, the particle will not be reflected, *i.e.* it would go through the neck of the magnetic bottle. That is, the  $90^\circ$  angle determines whether the particle is reflected or it goes through the bottleneck. Therefore, in the left-hand-side of Eq. (19), we can substitute the pitch angle by  $90^\circ$ . We can consider that, in this case, the corresponding angle at  $B_0$ , further referred to as  $\theta_{C0}$ , is the critical angle that makes the particle to be reflected and (and it will not pass through the region with  $B_m$ ). Then, it results the next equality

$$\frac{\sin^2 90^\circ}{B_m} = \frac{\sin^2 \theta_C}{B_0}. \quad (22)$$

We remember that if a particle has an initial pitch angle  $\theta_{C0}$  (in the zone of minimum  $B$ ) it will have a larger pitch angle as it moves to zones with larger magnetic fields. We then remark that the critical angle  $\theta_{C0}$  refers to the pitch angle of the particle in the region of the minimum magnetic field  $B_0$ , since for smaller angles at that region of  $B_0$ , a particle will go through the bottleneck at the region with  $B_m$ . It is worth to also remark that for  $\theta_{C0}$ , and larger pitch angles (at the region of  $B_0$ ), a particle will be reflected (at the region of  $B_m$ ). This is the reason because it is called a magnetic mirror [1].

Substituting the value of  $90^\circ$  (the condition to be reflected), we have that the critical angle condition requires that the pitch angle at the minimum magnetic field will be expressed based on a relation between the minimum and maximum magnetic field

$$\frac{B_0}{B_m} = \sin^2 \theta_{C0}. \quad (23)$$

Further, to analyze the situation of particle reflection as a function of the  $B_0/B_m$  ratio, in Fig. 2 we show two cases of the angle  $\theta_{C0}$  for two different ratios where  $B_{m1} > B_{m2}$ . We assume that the minimum magnetic field is the same in both cases.

In the other case, the maximum magnetic field on the left-hand-side is larger than that on the right-hand-side. Then, the initial angle that the particles should have, to pass through the neck of the magnetic bottle, is smaller in the case of the greater  $B_m$  value (left-hand-side) than the angle they require (to pass) in the case of the smaller  $B_m$  (represented on the right-hand-side). In other words, some particles passing through the neck of the bottle with weaker  $B_m$  (represented on the right-hand-side) would not pass (with the same angle of inclination) through the neck of the bottle with stronger  $B_m$  (left-hand-side).

The grey triangle of Fig. 2 represents the range of angles (at  $B_0$ ), where a particle should be directed to be lost (considering arrows whose back extreme is at the triangle apex on the left). It means, the triangles represent the initial pitch angle range at  $B_0$ , for which a particle will be able of passing through the magnetic neck. On the left-hand-side, the arrows

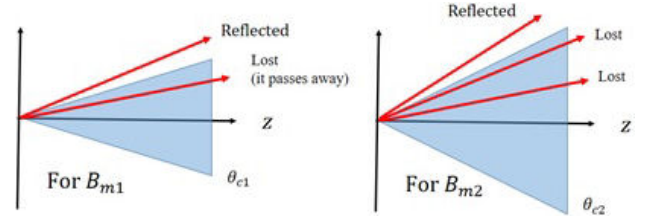


FIGURE 2. Representation of the range of angle of loss for two different  $B_0/B_m$  ratios, where  $B_0$  is the same for both cases and  $B_{m1} > B_{m2}$ . The arrows represent the pitch angles that different particles have in the zone of the minimum magnetic field  $B_0$ . The triangles represent the regions where the initial pitch angle of a particle should be directed to pass through the magnetic bottleneck (*i.e.* when it reaches the zone of the maximum magnetic field  $B_m$ ).

that are superimposed to the triangle will go through the magnetic neck. On the other hand, the arrow also on the left-hand-side plot, that is not superimposed to the triangle will be reflected, as indicated with a label in Fig. 2. The third arrow, from bottom to top, on the right-hand-side plot is at the same angle  $\theta$  than the third arrow at the left-hand-side. It means, they represent the same pitch angle.

We recall that the maximum magnetic fields are assumed such that  $B_{m1} > B_{m2}$  (and consequently  $[1/B_{m1}] < [1/B_{m2}]$ ). Then, from the triangles that represent particle loss in Fig. 2, one can clearly see that the smaller the  $B_0/B_m$  ratio, the smaller the pitch angle  $\theta_{C0}$  that a particle should have, in order to pass through the magnetic neck. As can be seen from the previous analysis, the relationship in Eq. (23) is clue to understand the reflection and loss in a magnetic bottle.

### 3. Montecarlo simulations

We made Montecarlo simulations to see how are the amounts of particles reflected as a function of the initial pitch angles. A number of 5,000 random pitch angles are used for the charged particles with values that follow a Gaussian distribution with a given central value (which is selected as zero) and a given Standard Deviation  $\sigma$ .

Simulations are made for different values of  $\sigma$ , in order to see how the amount of particles reflected varies with growing  $\sigma$ . Also, various  $B_0/B_m$  ratios are used (0.55, 0.40, 0.20, 0.13, and 0.10). A total velocity that corresponds to a given mean temperature  $T$  is used for all the particles.

As described in Sec. 2, the loss or reflection of a particle in a magnetic bottle depends only on the pitch angle that the particle has in the region of the weakest magnetic field. Let us remember that, if the value of the initial pitch angle  $\theta_{C0}$ , for a charged particle, is greater than  $\sin^{-1}(B_0/B_m)^{1/2}$  [Eq. (23)], then the particle is reflected. In order to study the influence of the standard deviation of the pitch angle distribution, which we call  $\sigma$ , on the reflection of the particles in the magnetic mirror.

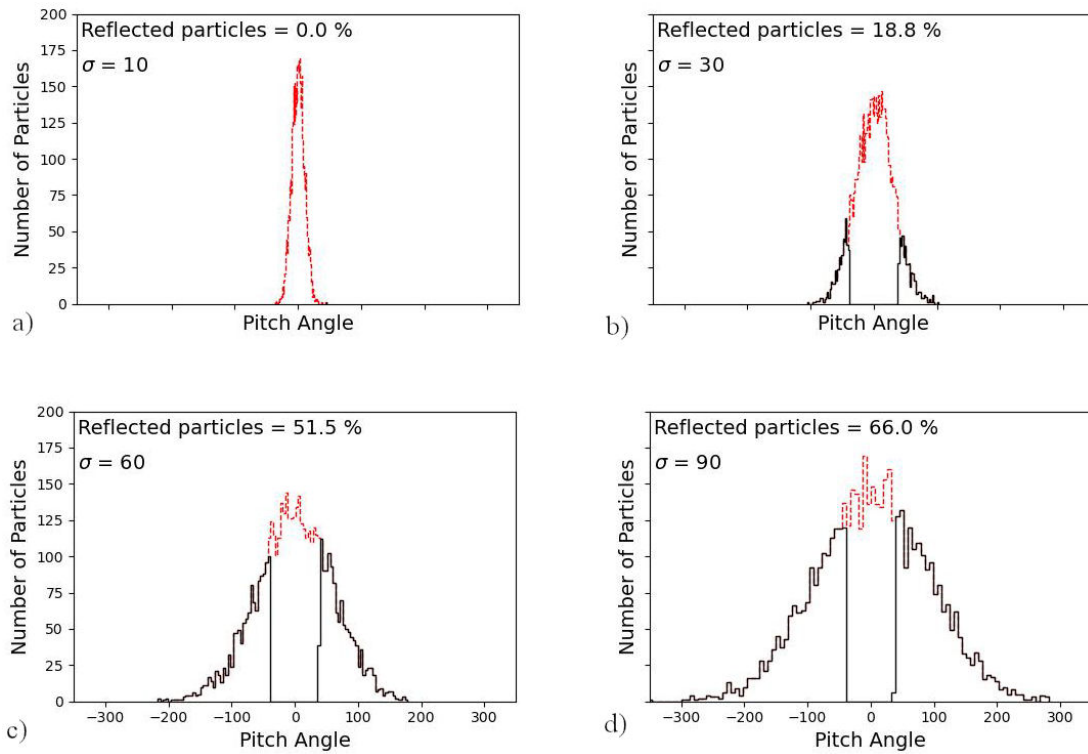


FIGURE 3. Histograms of the initial (dashed line) and final (continuous line) pitch angle distributions of electrons moving inside a magnetic bottle for  $B_0/B_m = 0.40$ . Each panel corresponds to a different value of  $\sigma$ , as indicated with a label. Also, for each case, the percent of reflected particles is given inside the given panel.

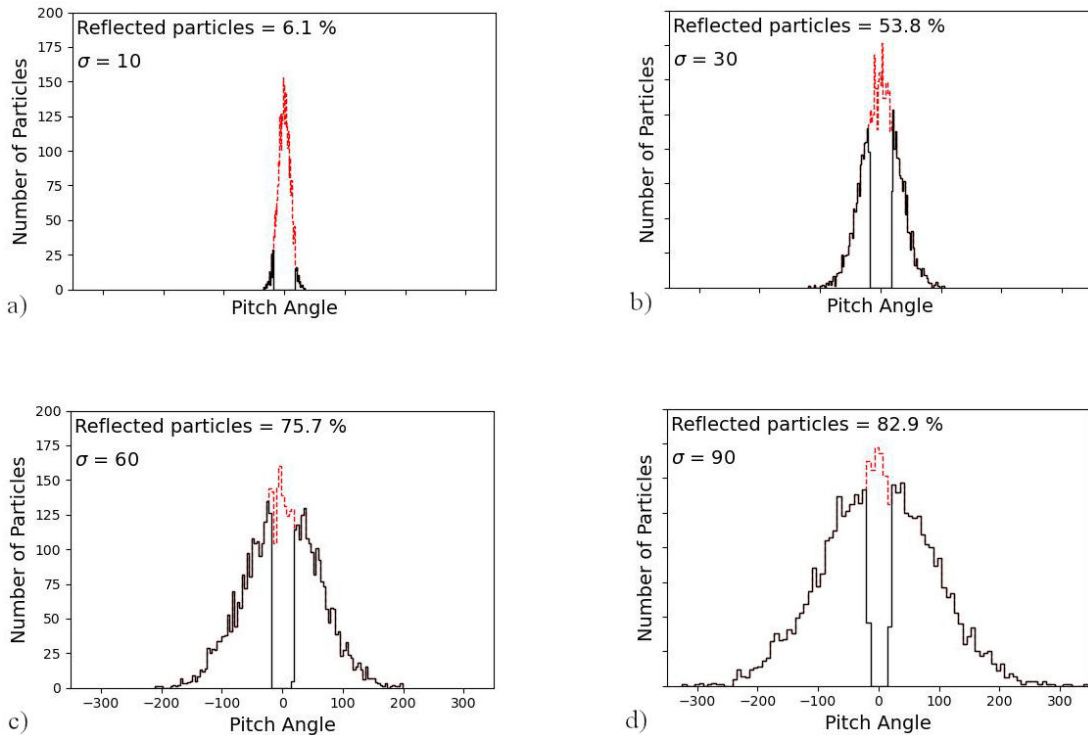


FIGURE 4. Histograms of the initial (dashed line) and final (continuous line) pitch angle distributions. In this case, for  $B_0/B_m = 0.10$ , which is a smaller ratio than that used to make the plots of Fig. 3. Provided that  $B_0$  is the same in both cases, the maximum magnetic field ( $B_m$ ) for the plots of the present figure has to be larger than the maximum magnetic field for Fig. 3. For this reason, the percent of reflected particles is larger in this case than in Fig. 3.

## 4. Results and discussion

We performed a number of simulations of initial pitch angle distributions with different values of  $\sigma$ .

As examples, the initial pitch angle distribution and the distributions of reflected electrons for  $\sigma = 10^\circ, 30^\circ, 60^\circ$  and  $90^\circ$  are shown for  $B_0/B_m$  ratios: 0.40 and 0.10 in Figs. 3 and 4, respectively. In each of them, two distributions are shown, one of them corresponds to the initial pitch angles in the sample (dashed line), and of the reflected particles (continuous line).

The plots correspond to two different cases of the magnetic field ratio [Eq. (23)]. In each case, the minimum magnetic field  $B_0$  can be considered the same, being the maximum magnetic field,  $B_m$ , different from one case to the other.

From Figs. 3 and 4, it can be seen that the percent of reflected particles depends on both, the  $B_0/B_m$  ratio and the standard deviation of the pitch angle distribution  $\sigma$ .

The percent of reflected particles grows with  $B_m$ , it means, it grows as the  $B_0/B_m$  ratio decreases. Also, particles at some angles that would pass, through the neck bottle, in the case of the larger  $B_0/B_m$  ratio, will be reflected for the case of the smaller ratio (see Fig. 2). For this reason, in the distributions of  $B_0/B_m = 0.10$  the gap in the middle of the reflected particles distributions is thinner than for the  $B_0/B_m = 0.40$  distributions. It means, some particles that for given angles can pass through the bottle for the  $B_0/B_m = 0.40$  ratio, are reflected for the  $B_0/B_m = 0.10$  one.

As expected from the theoretical analysis made in Sec. 2, the distributions made with the smallest  $\sigma$  lead to the largest

percent of passing particles (and a small percent of reflected ones).

For the plotted  $B_0/B_m$  ratios, the lowest percent of reflected particles ( $< 7\%$ ) takes place for  $\sigma = 10^\circ$ . For this  $\sigma$ , the percents go from 0 (for 0.40) to 6% (for 0.10). The percent of reflected particles reaches the highest values, between 83% and 84%, for  $\sigma = 90^\circ$ .

In Fig. 5, we plot the percents of reflected particles against  $\sigma$  (including some other  $\sigma$  to that shown at Figs. 3 and 4) for different values of the magnetic field ratios (also including  $B_0/B_m = 0.55$ , which is a higher value than those of Figs. 3 and 4).

As we have seen in the description of the  $B_0/B_m$  ratio, and its relation to the critical angle for reflection, the smaller this ratio, the larger will be the percent of reflected particles. It means, to have more particles reflected, the value of  $B_m$  should be as larger as possible in comparison to  $B_0$ .

As may be seen in Fig. 5, the number of reflected particles increases very rapidly, with increasing  $\sigma$ , in the range of  $10^\circ$  to  $40^\circ$ . For example, for a magnetic field ratio of 0.1, the percent of trapped particles increases by approximately 500% as  $\sigma$  increases from  $10^\circ$  to  $30^\circ$ .

For the other ratios, the increase is also large in this range of  $\sigma$ , but the amount of reflected particles is smaller as  $B_0/B_m$  increases (*i.e.* as the  $B_m$  value is weaker). If the purpose of the bottle would be to retain a large number of electrons, the option to avoid large magnetic fields is to increase the standard deviation of the pitch angle distribution, since this allows increasing the percentage of particles whose angle is greater than the critical angle.

## 5. Conclusions

The value of  $\sigma$  plays an important role to make the particles being reflected, for the different  $B_0/B_m$  ratios here studied. It is found that the number of reflected particles increases very rapidly with  $\sigma$ , in the range of  $10^\circ$  to  $40^\circ$ .

From  $10^\circ$  to larger  $\sigma$ , the difference in the percent of reflected particles is clear ( $> 5\%$ ) for all the  $B_0/B_m$  ratios. For example, for the  $\sigma$  range from  $20^\circ$  to  $40^\circ$ , the percent of reflected particles is  $\gtrsim 20\%$  larger for  $B_0/B_m = 0.10$  (*i.e.* for the largest  $B_m$ ) than for the 0.55 ratio (which corresponds to the lowest  $B_m$ ).

## Acknowledges

We are grateful to the anonymous referee, who carefully reviewed our paper and made suggestions that allowed us to identify how to change the content and make other modifications to improve it. Fernandez-Ramos L.A. and Tirado-Bueno E. want to thank CONAHCYT for the postgraduate grant. All authors thank the INAOE supercomputing laboratory for the time allocated to do a series of simulations that served to obtain some of the results presented in this work.

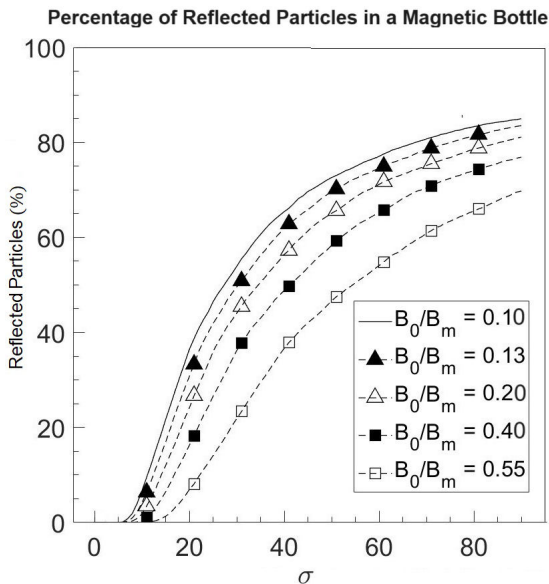


FIGURE 5. Percents of reflected particles against  $\sigma$ . Each curve corresponds to a given magnetic field ratio, which is given in the inserted panel.

- 
1. M.-B. Kallenrode, *Space Physics: An Introduction to Plasmas and Particles in the Heliosphere and Magnetospheres*, 3rd ed. (Springer Berlin, Heidelberg, 2004). <https://doi.org/10.1007/978-3-662-09959-9>.
  2. O. Al-Habahbeh *et al.*, Review of magnetohydrodynamic pump applications, *Alex. Eng. J.* **55** (2016) 1347, <https://doi.org/10.1016/j.aej.2016.03.001>.
  3. F. F. Chen, *Introduction to Plasma Physics and Controlled Fusion*, 3rd ed. (Springer Cham, 2016), <https://doi.org/10.1007/978-3-319-22309-4>.
  4. R. P. H. Goldston, R.J., *Introduction to plasma physics*, 1st ed. (CRC Press, 1995).
  5. W. Baumjohann and R. A. Treumann, *Basic Space Plasma Physics*, 3rd ed. (WORLD SCIENTIFIC, 2022), <https://doi.org/10.1142/12771>.
  6. R. H. Goddard, (Clark University Archive).